Passive Pressure on Skewed Bridge Abutments

Pression passive sur des culées de pont asymétriques

Jessee S.
Terracon Consultants, Oklahoma City, Oklahoma, USA

Rollins K.
Brigham Young University, Provo, Utah, USA

ABSTRACT: The passive force-deflection relationship for abutment walls is important for bridges subjected to thermal expansion and seismic forces. Although a number of tests have been performed to investigate these relationships for non-skewed abutments, no tests have been performed for skewed abutments. To determine the influence of skew angle on the development of passive force, lab tests were performed on a wall with skew angles of 0º, 15º, 30º, and 45º. The wall was 1.26 m wide and 0.61 m high and the backfill consisted of dense compacted sand. As the skew angle increased, the passive force decreased substantially with a reduction of 50% at a skew of 30º. An adjustment factor was developed to account for the reduced capacity as a function of skew angle. The horizontal displacement necessary to develop the peak passive force was typically about 2.5 to 3.5% of the wall height, H, and the residual passive force typically dropped by 40% at a deflection of 4 to 6% of H. For the no-skew case, the shape of the failure plane closely resembled that predicted by the Rankine theory but was much shorter than that predicted by the log-spiral approach. Nevertheless, the log-spiral method accurately predicted the measured force while the Rankine method grossly under predicted the force.

RÉSUMÉ: La relation force- déformation passive des murs en retour est importante pour les ponts soumis à la dilatation thermique et des forces sismiques. Bien qu'un certain nombre de tests aient été réalisés afin d'étudier ces relations pour les murs non-biais, aucun test n'a été effectué pour les murs biais. Pour déterminer l'influence de l'angle du biais sur le développement de la force passive, des tests de laboratoire ont été effectués sur un mur ayant des angles de 0 º, 15 º, 30 º et 45 º. Le mur a une largeur de 1.26 m et 0.61 m de hauteur, le remblai se compose de sable compacté. Lorsque l'angle du biais augmente, la force passive diminue considérablement avec une réduction de 50% pour un biais de 30º. Un facteur d'ajustement a été mis au point pour tenir compte de la réduction de capacité en fonction de l'angle du biais. Le déplacement horizontal nécessaire pour développer la force maximale passive est généralement d'environ de 2.5 à 3.5% de la hauteur du mur H, et la force résiduelle passive chute généralement de 40% pour un biais de 4 à 6% de H. Pour les cas non-biais, la forme du plan de rupture est proche de celle prévue par la théorie de Rankine, mais beaucoup plus courte que celle prédite par la méthode de la spirale logarithmique. Néanmoins, la méthode de la spirale logarithmique prédit avec précision la force mesurée alors que la méthode de Rankine sous-évalue largement la force.

KEYWORDS: Passive force, Passive Pressure, Skewed abutments, Earth pressure, Dense sand, Plane Strain, Log-Spiral.

1 INTRODUCTION

The passive force-deflection relationship for abutment walls is important for bridges subjected to thermal expansion and seismic forces. Although a number of tests have been performed to investigate these relationships for non-skewed abutments (Maroney 1995, Duncan and Mokwa 2001, Rollins and Cole 2006, Rollins and Sparks 2002, Lemnitzer et al 2009), no tests have been performed to investigate these relationships for skewed abutments. Performance of skewed bridges during the 2010 M8.8 Chilean earthquake suggests that this may be an issue of concern as several such bridges were observed to have rotated about a vertical axis, becoming unseated in their acute corners (EERI, 2010).

While current design codes (AASHTO 2011) consider that the ultimate passive force will be the same for a skewed abutment as for a non-skewed abutment, numerical analyses performed by Shamsabadi et al. (2006) indicate that the passive force will decrease substantially as the skew angle increases. Reduced passive force on skewed abutments would be particularly important for bridges subject to seismic forces or integral abutments subject to thermal expansion. To better determine the influence of skew angle on the development of passive force, a series of large size laboratory tests were performed on a wall that was 1.26 m (4.1 ft) wide and 0.61 m (2 ft) high. A dense sand was compacted behind the wall to simulate a bridge approach fill. Passive force-deflection curves were measured for skew angles of 0º, 15º, 30º, and 45º. Vertical columns of red soil were embedded into the backfill sand so that the failure surface could be located at the completion of the testing. This paper describes the test program, the test results, and the implications for design practice based on analysis of the test results.

1 BACKGROUND

The distribution of forces at the interface between a skewed bridge and the adjacent backfill soil is illustrated in Fig. 1 as originally outlined by Burke (1994). The longitudinal force (P_L) can be induced by thermal expansion or seismic forces. For static or simplified pseudo-static analyses, the components of the longitudinal force normal and transverse to the abutment must be resisted by the passive force (P_p) normal to the abutment backwall and the shear resistance (P_R) on the backwall. Summing forces normal to the abutment produces the equation

$$P_p = P_L \cos\theta \quad (1)$$

where θ is the skew angle of the backwall.

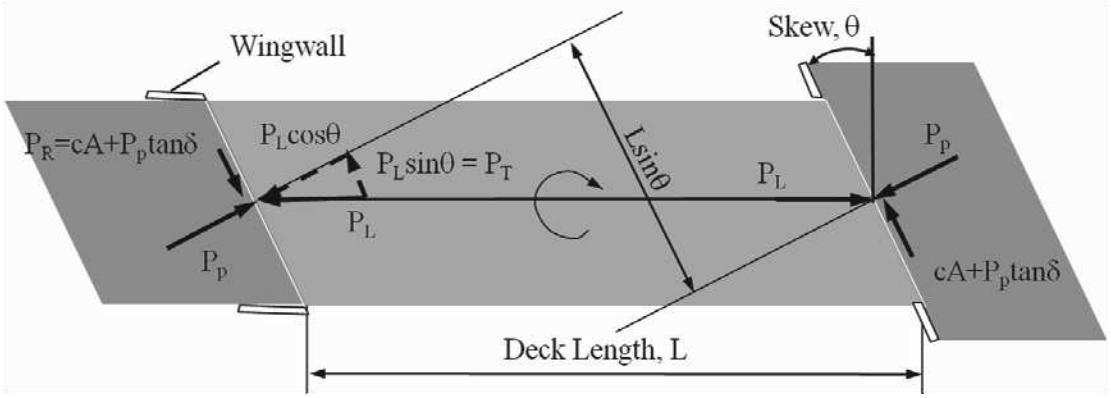

Figure 1. Illustration of forces acting on a skewed bridge at the soil-abutment interface

The transverse applied shear force (P_T) can be computed using the equation

$$P_T = P_L \sin\theta \quad (2)$$

while the transverse shear resistance (PR) can be given by the equation

$$P_R = cA + P_P \tan\delta \quad (3)$$

Summing forces transverse to the backwall produces the equation

$$(cA + P_P \tan\delta)/Fs \geq P_L \sin\theta \quad (4)$$

where c is the soil cohesion, A is the area of the backwall, δ is the angle of wall friction between the backfill soil and the concrete abutment backwall, and Fs is a factor of safety. If the applied transverse shear resistance exceeds the ultimate shear resistance, the abutment could slide against the soil leading to an unstable condition.

In addition, the offset in passive force on the abutments produce a force couple which must be resisted by the force couple produced by the shear resistances on each abutment. Summing moments about a vertical axis leads to the equation

$$(cA + P_P \tan\phi)\, L \cos\theta/Fs \geq P_P\, L \sin\theta \quad (5)$$

Again, if the shear resistance is insufficient, the bridge will tend to rotate, which would likely change the distribution of passive force on the abutments. Based on Eq 5, Burke (1994) suggested that rotation would be expected for skew angles greater than 15º with smooth abutment-soil interfaces and no cohesion as the factor of safety dropped from 1.5 to 1.0. If cohesion is ignored, the potential for rotation is independent of both P_p and the length of the bridge, L.

2 TEST LAYOUT

The test layout is illustrated in Fig. 2. A concrete wall 1.26 m (4.13 ft) wide and 0.61 m (2 ft) high was used to model the backwall of an abutment. Passive force-deflection tests were performed with skew angles (θ) of 0º, 15º, 30º, and 45º. Two tests were performed for each skew angle to evaluate repeatability. A dense sand was compacted behind the wall to simulate the backfill in a typical approach fill. The sand backfill was 0.9 m (3 ft) thick and extended 0.3 m (1 ft) below the base of the wall. The backfill was 3 to 4 m (10 to 13 ft) long to completely contain the failure surface and was slightly wider than the wall 1.28 m (4.21 ft) to allow the backwall to move into the sand backfill without any friction on the concrete sidewall. To support the sand backfill during compaction, two 1.5 m concrete blocks were bolted to the structural floor of the laboratory on either side of the fill near the wall. Beyond the concrete blocks, plywood walls were braced into a vertical position. Two plastic sheets were placed along the sidewalls of the backfill to create a low friction surface and produce a 2D or approximately plane strain geometry. A base was constructed below the concrete backwall and rollers were placed at the interface between the backwall and the base to provide a normal force but minimize base friction.

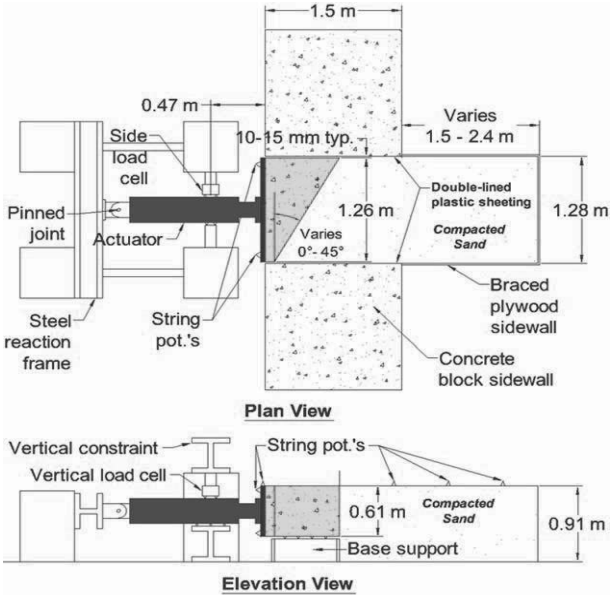

Figure 2. Plan and elevation views of the test layout.

Tests were performed by pushing the backwall longitudinally into the backfill sand using a 490 kN (110 kip) hydraulic actuator which was bolted to the backwall. Load was applied at a rate of 0.25 mm/min (0.1 inch/min); but sand is not very rate sensitive. Vertical and horizontal load cells were mounted between the reaction frame and the actuator so that the loads necessary to hold the wall in place could be measured.

2.1 *Instrumentation*

Load was measured by pressure transducers in the actuator. To measure the movement of the backwall, four longitudinal string potentiometers were positioned at the corners of the wall and two transverse string pots were positioned at the top and bottom of one side. In addition, a final string pot was used to monitor the vertical movement.

The position of the failure surface was monitored by marking 0.3 m (1 ft) square grids at the backfill surface. The subsurface failure plane position was located by placing vertical

columns of red sand spaced along the longitudinal axis behind the wall.

2.2 *Backfill soil properties*

The sand backfill is clean poorly-graded sand classifying as SP according to the Unified Soil Classification System and A-1-b according to the AASHTO system. The particle size distribution curve falls within the gradation limits for washed concrete sand (ASTM C33) with Cu of 3.7 and Cc of 0.7. A modified Proctor test was performed on the sand and indicated a maximum dry unit weight of 17.8 kN/m3 (113.5 lbs/ft3). The sand was placed in 150 mm (6 in) lifts and the average relative compaction achieved was typically about 98%.

Load testing was generally performed two days after compaction and moisture content measurements at various depths were made immediately after testing. These measurements indicated good consistency between tests, with the moisture content typically falling within 7 to 9%.

Based on a direct shear test the drained friction angle (φ') was found to be 46º with a cohesion of 7 kPa (140 psf). Interface friction tests were also performed between the sand and the concrete and a wall friction angle (ϕ) of 33º was measured.

Because the compacted sand in a partially saturated state could be excavated with a vertical face and remained stable for long periods, the potential for apparent cohesion owing to matric suction was also investigated. Suction measurements indicated that the sand at the moisture content during testing had a matric suction (ψ) (negative pressure relative to atmospheric pressure) of approximately 4 to 5 kPa (80 to 100 psf). Based on recommendations of Likos et al (2010), this magnitude of suction produces an apparent cohesion (ca) of approximately 4 to 5 kPa (80 to 100 psf).

3 TEST RESULTS

3.1 *Passive force-deflection curves*

The passive force versus longitudinal deflection curves for the tests at each of the skew angles are plotted in Fig. 3. Although the initial stiffness for each curve is remarkably similar, the peak passive force clearly decreases as the skew angle increases. In addition, there appear to be some differences in the shape of the passive force displacement curves as skew angle increases.

The passive force-deflection curve appears to exhibit a typical hyperbolic curve shape for the no skew case however, it transitions to a different shape as the skew angle increases. As the skew angle increases, the passive force exhibits a longer plateau where the force remains relatively constant or increases gradually with deflection before reaching a peak and abruptly decreasing to a residual value. The peak passive force typically developed at a normalized deflection of 2.5% to 3.5% of the wall height (H), and did not change consistently with skew angle. The tests typically showed a reduction in the passive force to a residual value at a normalized displacement of 0.04H to 0.06H. The post-peak residual strength ranged from 53 to 72% of the peak value with an average of 60%.. This decrease in post peak resistance is consistent with results from the direct shear tests.

The peak passive force for each test at a given skew angle has been divided by the peak passive force at zero skew and the results are plotted as a function of skew angle in Fig. 4. Normalized data from numerical analyses of skew abutments reported by Shamsabadi et al (2006) are also shown in Fig. 4 and the results follow the same trend line. The curve has been extrapolated to zero at a skew angle of 90°. The no skew case involves pure passive resistance and zero shear force. A skewed wall is subject to a combination of both passive resistance and side shear force. At the largest possible skew angle, 90°, the forces acting on the wall transition to pure side shear force with zero passive resistance.

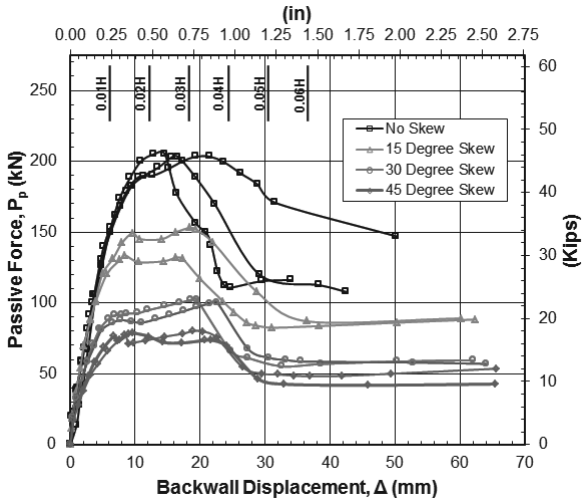

Figure 3. Passive force versus longitudinal backwall displacement for the tests at each skew angle.

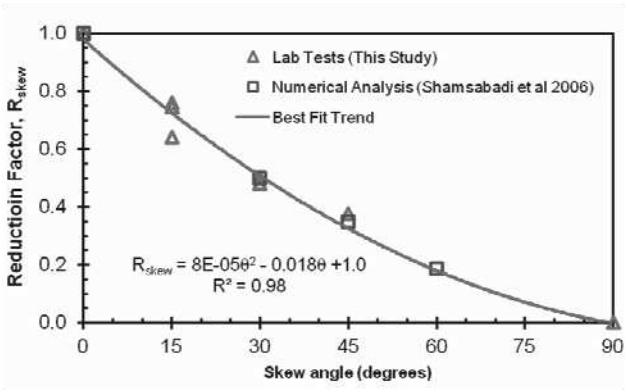

Figure 4. Normalized peak passive force versus skew angle from lab tests and numerical model results.

As indicated previously, vertical and horizontal displacements of the wall during the tests were minimal. Wall displacement was less than 4.4 mm for vertical movement and less than 2.3 mm for transverse movement for the skew angles tested.

3.2 *Failure surface geometry*

The failure surface for the no skew case was approximately the same length across the width of the sand box; however, when a skew angle was involved, the failure surface also exhibited a skew across the width of the sand box. The failure surface did not manifest itself at the ground surface until after the peak force had been reached.

The failure surface within the sand was clearly identifiable from the offset in the red sand columns. The failure surface geometry is shown as a function of distance behind the middle of the wall for the various skew angles in Fig. 5. In addition, the ground surface heave is also plotted for each test. The average length of the failure surface behind the middle of the wall was 2.1 m (7.0 ft) with a standard deviation of 0.3 m (1.0 ft). The length of the failure surface ranged from 1.8 to 2.6 m (5.9 to 8.6 ft). The failure surface typically extended 75 mm to 300 mm. horizontally from the bottom of the wall then exhibited a relatively linear trend line upward to the surface. The angle of inclination of the trend line was between 19º and 21.5º with an average of 20°. Assuming that the angle of inclination (α) of the straight line segment of the log-spiral failure wedge is given by the equation:

$$\alpha = 45 - \varphi'/2 \quad (8)$$

as suggested by Terzaghi and Peck (1948), then the interpreted drained friction angle would be between 47º and 52º with an average of 50º. The inferred friction angle value is higher than the measured friction angle from the direct shear test, but is close the value that would be expected for the plane strain friction angle. The conditions and geometry of the sand box simulated a plane strain condition as well. Based on a number of studies, Kulhawy and Mayne (1990) determined that the plane strain friction angle for dense sand was 11% higher than the triaxial value on average. Thus, the plane strain friction angle for the sand used in the tests would be about 51°, which is approximately the same value as that of the inferred friction angle from the inclination of the failure wedge.

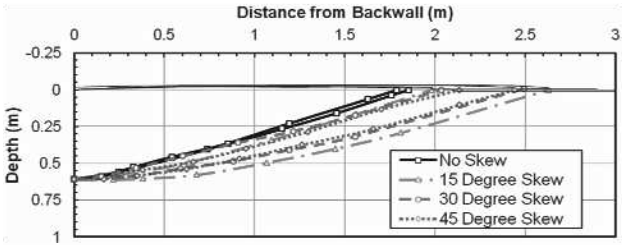

Figure 5. Measured failure surface depth versus distance from the backwall for each test.

4 ANALYSIS OF RESULTS

Test results were analyzed using the Rankine (1857) and log-spiral (Terzaghi, 1948) passive pressure theories. Table 1 shows comparisons of the test results with computed passive force and failure surface orientation for the no-skew case. The measured and theoretical failure surface geometries for the no-skew case relative to the top of the wall are shown in Fig. 6. For the analysis, the soil friction angle was taken as 50°, consistent with the plane strain value, with a cohesion of 4.5 kPa (90 psf), and the wall friction angle was taken as 33° based on interface tests. While the failure plane according to the log-spiral method generally exceeded the length of the failure surface by 45 to 50%, this method was most effective in computing passive force. In contrast, the Rankine method grossly underestimated the measured force, but gave a reasonable approximation of the failure surface geometry. Although the Coulomb theory is widely used, it is limited to cases where δ/φ is less than about 0.5. For these tests, δ/φ is equal to 0.66. Thus, analyses using the Coulomb method predict an unreasonably high value for the passive force, and the failure surface extent is likewise unreasonably over-predicted (see Table 1).

5 CONCLUSIONS

1. Large scale laboratory tests and numerical analyses indicate that the peak passive force for a skewed abutment significantly decreases as the skew angle increases. Based on available results, this reduction can be accounted for by using a simple reduction factor. This reduction may be dependent on abutment geometry and other unknown factors and should thus be used with caution until further research is performed.
2. For the dense sand typical of approach fills, the peak passive force for all tests typically developed at longitudinal deflections between 0.025H and 0.035H. However, the shape of the passive force-deflection curve up to the peak value transitioned from a typical hyperbolic shape for the no skew case to a bilinear shape for the skewed walls.
3. At wall displacements beyond the peak (0.04 to 0.06H) the passive force decreased substantially and the residual force was typically about 40% below the peak force, which is in agreement with the behavior in the direct shear tests.
4. Based on the measured soil parameters the log spiral method provided the best agreement with the measured passive force, while the Rankine method grossly underestimated the force. However, the failure surface geometry was closer to that predicted by the Rankine method than the log spiral shape.

Table 1. Summary of measured tests results in comparison with computed values using different passive pressure theories.

	Passive Force		Failure Surface Geometry	
	(kN)	*% of measured*	*Orientation* (degrees)	*Extent* (m)
Avg. Measured	205 (46 kips)	100	20	1.8 (6.0 ft)
Coulomb Theory	1115 (251 kips)	545	3.4	10 (33 ft)
Rankine Theory	51 (12 kips)	25	20	1.8 (5.8 ft)
Log-Spiral Theory	205 (46 kips)	100	-	3.1 (10 ft)

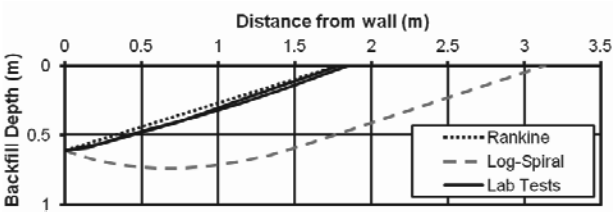

Figure 6. Measured and theoretical failure surface geometries for the no-skew case.

6 REFERENCES

AASHTO (2011), Guide Specifications for LRFD Seismic Bridge Design, 2nd Edition. 286 p.

Burke, M.P. Jr. (1994). "Semi-Integral bridges: movements and forces". Transportation Research Record 1460, Transportation Research Board, Washington, D.C., p. 1-7.

Cole, R.T and Rollins, K.M. (2006). "Passive Earth Pressure Mobilization During Cyclic Loading." *J. Geotech.& Geoenviron. Eng*, ASCE, 132(9), 1154-1164.

Duncan, J. M., and Mokwa, R. M. (2001). "Passive earth pressures: theories and tests." *J. Geotech. & Geoenv.l Engrg.,* ASCE Vol. 127, No. 3, pp. 248-257.

EERI (2010). "The M_w 8.8 Chile Earthquake of February 27, 2010". EERI Special Earthquake Report. June, 2010.

Kulhawy, F. H., and Mayne, P. W. (1990). "Manual on estimating soil properties for foundation design." Research Project 1493-6, EL-6800, Electric Power Research Institute. Palo Alto, California.

Lemnitzer, A., Ahlberg, E.R., Nigbor, R.L., Shamsabadi, A., Wallace, J.W., and Stewart, J.P. (2009). "Lateral performance of full-scale bridge abutment wall with granular backfill," *J. Geotech. & Geoenv. Engrg.*, ASCE, 135 (4), 506-514.

Likos, W.J. Wayllace, A., Godt, J., and Ning, L. (2010). "Direct shear apparatus for unsaturated sands at low suction and stress". Geotech. Testing J., ASTM, 33(5)

Maroney, B.H. (1995) "Large scale abutment tests to determine stiffness and ultimate strength under seismic loading" Ph.D. Dissertation, Civil Engineering Dept., University of California, Davis.

Rankine, W. J. (1857). On the stability of loose earth. *Philosophical Transactions of the Royal Society of London, 147*.

Rollins, K.M. and Cole, R.T. (2006). "Cyclic Lateral Load Behavior of a Pile Cap and Backfill." *J. Geotech. & Geoenviron. Eng*., ASCE, 132(9), 1143-1153.

Rollins, K.M. and Sparks, A.E. (2002) "Lateral Load Capacity of a Full-Scale Fixed-Head Pile Group." *J. Geotech. & Geoenviron. Eng*., ASCE, Vol. 128, No. 9, p. 711-723.

Shamsabadi, A. Kapuskar, M. and Zand, A. (2006). "Three-dimensional nonlinear finite-element soil-Abutment structure interaction model for skewed bridges". 5th National Seismic Conf. on Bridges and Highways, FHWA, p.

Terzaghi K. and Peck, R. B. (1948). Soil Mechanics in Engineering Practice, John Wiley and Sons, New York, p.